

Fermi Surface of 3d<sup>1</sup> Perovskite  $\text{CaVO}_3$  Near the Mott TransitionI. H. Inoue,<sup>1,2</sup> C. Bergemann,<sup>3</sup> I. Hase,<sup>4</sup> and S. R. Julian<sup>3</sup><sup>1</sup>Correlated Electron Research Center (CERC), AIST Tsukuba Central 4, Tsukuba 305-8562, Japan<sup>2</sup>IRC in Superconductivity, University of Cambridge, Madingley Road, Cambridge CB3 0HE, UK<sup>3</sup>Cavendish Laboratory, University of Cambridge, Madingley Road, Cambridge CB3 0HE, UK<sup>4</sup>Nanoelectronics Research Institute, AIST Tsukuba Central 2, Tsukuba 305-8568, Japan

We present a detailed de Haas van Alphen effect study of the perovskite  $\text{CaVO}_3$ , offering an unprecedented test of electronic structure calculations in a 3d transition metal oxide. Our experimental and calculated Fermi surfaces are in good agreement (but only if we ignore large orthorhombic distortions of the cubic perovskite structure). Subtle discrepancies may shed light on an apparent conflict between the low energy properties of  $\text{CaVO}_3$ , which are those of a simple metal, and high energy probes which reveal strong correlations that place  $\text{CaVO}_3$  on the verge of a metal-insulator transition.

PACS numbers: 71.18.+y, 71.20.-b, 71.30.+h

Transition metal oxides (TMOs) have for many decades been a rich source of novel and intriguing electronic behaviour. The narrow bands in the 3d TMOs are particularly susceptible to correlation effects, leading to phenomena as unexpected and diverse as high temperature superconductivity [1, 2], colossal magnetoresistance [3], and the recently discovered "orbitalons" in  $\text{LaMnO}_3$  [4, 5]. The Mott transition [6, 7] (a metal-insulator transition (MIT) driven by electron-electron interactions) lies at the heart of TMO physics, and the 3d<sup>1</sup> system  $\text{CaVO}_3$  is emerging as an important model compound that lies just on the metallic side of this transition [8, 9, 10, 11].

While the general principles involved in the MIT are probably understood, the predictive power of existing theories is poor when applied to real materials. On the one hand, models of the MIT that explicitly tackle dynamical many-body interactions use generic Hamiltonians that ignore the effects of real crystal structures; on the other, single-particle self-consistent band structure calculations based on the Local Density Approximation (LDA), which have had the most success at predicting the electronic structure of real metals, fail spectacularly in insulating TMOs such as  $\text{NiO}$  which is predicted by the LDA to be metallic. This problem is compounded by a lack of high quality data on the electronic structure of TMOs: for example until now the exclusive source of information on the Fermi surface geometry in TMOs has been angle resolved photoemission spectroscopy (ARPES), but this technique detects a much higher energy response than is observed in transport and thermodynamic measurements, and the results are frequently distorted by surface effects.

$\text{CaVO}_3$  is one of a series of 3d<sup>1</sup> perovskites that straddle the MIT. It is a metal, but large orthorhombic distortions of the cubic perovskite crystal structure and the spectroscopic properties of  $\text{CaVO}_3$  suggest that it lies very close to the MIT [8, 9, 10, 11]. Photoemission spectroscopy in  $\text{CaVO}_3$  appears to show: (a) the formation of

Hubbard bands [12, 13, 14, 15] | a precursor of the insulating state arising from strong electron correlation; and (b) a weaker spectral intensity at the Fermi energy  $E_F$  than is predicted by band structure calculations [12, 16]. From these and other measurements a broad picture is emerging of a striking conflict between low and high energy scales in  $\text{CaVO}_3$ , the former being revealed for example in specific heat measurements and suggesting that  $\text{CaVO}_3$  is a simple metal with small mass enhancements (normally a signature of weak electron-electron interactions), while the latter are probed by spectroscopic methods and show strong electron-electron interactions. The origin of this conflict is unclear. It may be an experimental artifact arising from enhanced sensitivity of spectroscopy to the surface as opposed to the bulk, but extra care has been taken to minimise this [16]. An intriguing suggestion is that the conflict, and the breakdown of the LDA that it implies, can be explained by a strong interaction that is non-local in space but local in time, such as for example the unscreened Coulomb interaction. But for this to occur, we require either a breakdown of screening in a material that at dc-frequencies at least has a normal metallic conductivity, or else a new non-local interaction such as might be mediated by orbital fluctuations.

Further experimental data are clearly needed, and this was the motivation for the present de Haas van Alphen (dHvA) effect study, which allows an unprecedented and detailed comparison between modern electronic structure calculations and an experimentally determined Fermi surface in a 3d TMO. It should be noted that LDA calculations have an excellent record predicting the Fermi surface shapes of even strongly correlated electron systems such as  $\text{UPt}_3$  [17], in which electron-electron interactions are enormously strong. This is probably because the Fermi volume is invariant under interactions [18]: volume conserving distortions of the Fermi surface require not only a k-dependent (i.e. spatially non-local) interaction [19] such as was invoked to explain the photoemission results, but also an anisotropic Fermi surface,

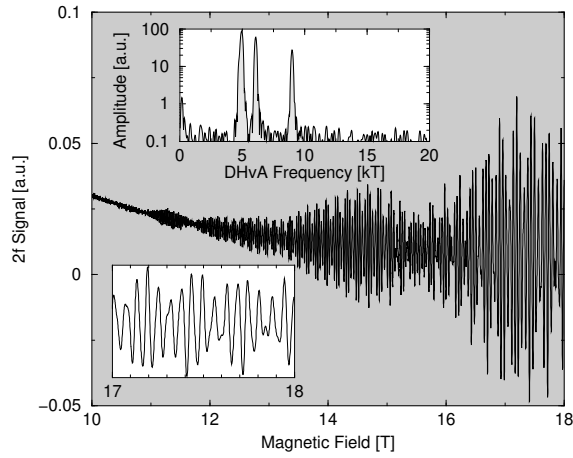


FIG. 1: Example of a dHvA field sweep on  $\text{CaVO}_3$  with the applied field parallel to the  $b$ -axis. The lower inset is a blow-up of the high-field region. The upper inset shows a logarithmic plot of the dHvA frequency spectrum, taken over the 18 T to 15 T field range.

so that states in different regions of the Fermi surface undergo different shifts in energy.

Quantum oscillations, such as the magnetisation oscillations in the de Haas-van Alphen (dHvA) effect, arise from the quantisation of cyclotron motion of charge carriers in a magnetic field. This provides the most detailed and the most reliable information about Fermi surface properties [20]. A prerequisite for the observation of the quantum oscillation effects is that quasiparticles must be able to complete a cyclotron orbit without scattering; this typically requires mean-free paths of  $\sim 1000 \text{ \AA}$  or more. It is this requirement of very high purity single crystals that has hitherto prevented quantum oscillations from being observed in 3d TMOs.

We used high-quality single crystals of  $\text{CaVO}_3$ , grown by the coating zone method yielding single-crystalline grains of typical size  $4 \times 4 \times 6 \text{ mm}^3$ . We kept the oxygen stoichiometry as small as possible by annealing the sample in air at  $150^\circ \text{C}$  for four days [8]. The oxygen stoichiometry of Ca and V was below the detectability limit (less than 1%) of an inductively coupled plasma atomic emission spectrometer. The  $\text{CaVO}_3$  crystals are orthorhombic ( $P_{nma}$ ) containing four  $\text{CaVO}_3$  formulae in the unit cell with lattice parameters  $a = 5.314 \text{ \AA}$ ,  $b = 7.521 \text{ \AA}$ ,  $c = 5.339 \text{ \AA}$  (Nakotte, H. & Jung, M.-H., private communication); the samples were oriented by Laue x-ray diffraction.

We have performed a thorough dHvA rotation study on two high-quality single crystals of  $\text{CaVO}_3$  ( $1 \times 1 \times 2 \text{ mm}^3$ , residual resistivity  $\rho_0 \sim 1.5 \text{ m}\Omega$ ) with the direction of the applied magnetic field  $B$  rotating in the ( $a$ - $b$ ) plane from  $b$  to  $a$ , and in the ( $a$ - $c$ ) plane from  $a$  to  $c$ . The experiments were carried out in a low-noise superconducting magnet system in field sweeps from 18 T to 10 T,

at temperatures down to 50 mK. A modulation field of 14.3 mT amplitude was applied to the sample, and the second harmonic of the voltage induced at the pick-up coil around the sample was recorded, essentially measuring  $\partial^2 M / \partial B^2$ .

A typical signal trace, demonstrating the high quality of our data, can be viewed in Fig. 1. The Fourier transform as a function of  $1/B$  gives the dHvA frequency spectrum, with peaks at a frequency  $F$  corresponding to extremal (i.e., maximum or minimum) FS cross-sectional areas  $S_m$  measured in planes perpendicular to  $B$ , via  $S = 2eF/h$ .

In Fig. 2, we present a density plot of the dHvA spectrum as a function of the direction of  $B$ , representing the information of about 100 field sweeps at angular intervals of  $2^\circ$ . In comparison, we have calculated the dHvA frequencies  $F_{\text{calc}}$  from four FS sheets (see Fig. 3) obtained by a band calculation using the computer code KANSAS I-94 with the LDA scheme [21] for the one-electron exchange-correlation potential. In the calculation, we used basis functions in  $|\mathbf{k} + \mathbf{G}\rangle$  with  $K_{\text{max}} = 620 (2/\text{\AA})$ , where  $\mathbf{k}$  is the wavevector and  $\mathbf{G}$  is a reciprocal lattice vector, to obtain about 1440 basis linear augmented plane waves; the core and valence states were calculated self-consistently by the scalar-relativistic scheme [22] with muffin-tin radii of 0.25 a for Ca, 0.20 a for V, and 0.14 a for O.

As seen in Fig. 2, there are very significant discrepancies between  $F_{\text{calc}}$  (thin dashed lines) and the experimental dHvA frequencies  $F_{\text{exp}}$  (grey-shaded). To list a few, (a) the 9 kT branches in  $F_{\text{exp}}$  have no correspondence in  $F_{\text{calc}}$ , and (b) the #63 sheet is not observed in  $F_{\text{exp}}$  unless we accept a deviation of about 20%. Only #64 and some of the orbits on #62 show satisfactory coincidence.

Although we observe this large discrepancy between experiment and LDA, we do not believe that this is the end of the story, because we have found that excellent agreement between theory and experiment can be regained if we ignore the orthorhombic distortion in the crystal structure, and recalculate the Fermi surface as though  $\text{CaVO}_3$  were cubic. We attempted to fit the calculated LDA bands of the orthorhombic lattice structure to a hypothetical "cubic" tight-binding (TB) Hamiltonian consisting of V  $3d_{xy}$ ,  $3d_{yz}$  and  $3d_{zx}$  orbitals, with nearest neighbour, next-nearest neighbour and hybridization matrix elements. Then, the results (thick solid lines in Fig. 2) show extremely good agreement with experiment: the differences in  $F$  are only 4% or less. As depicted in Fig. 3, in this assumption, the orthorhombic FS sheets #61, #62, and #63 will coalesce into the hypothetical "cubic" FS sheets and, while the #61 sheet remains unaffected. The sheet connects up with itself in the neighbouring BZ, forming a "jungle gym" type structure. The large hole orbit in this "jungle gym" explains the high-frequency features in  $F_{\text{exp}}$ , e.g. along the  $b$ -axis.

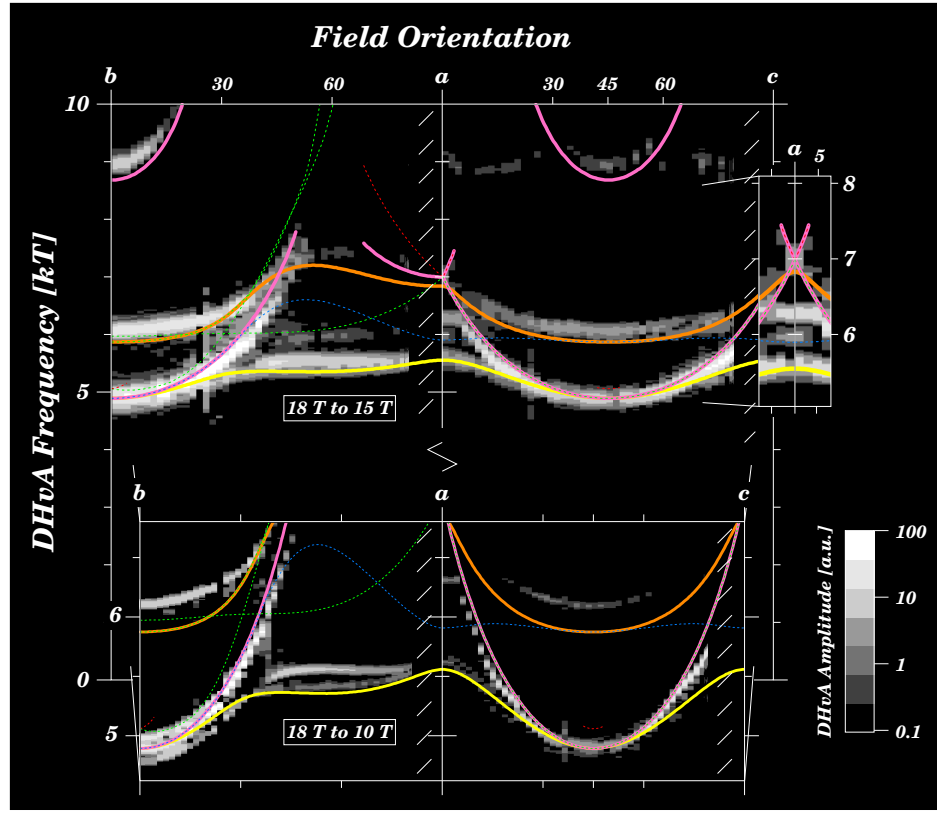


FIG. 2: Density plot of the dHvA spectrum of  $\text{CaVO}_3$  as a function of the direction of  $\mathbf{B}$  (greyshaded). The main panel uses the high-field (18 T ! 15 T) sections of each sweep, while the lower inset uses all available data (18 T ! 10 T), with higher frequency resolution at the expense of signal-to-noise. The right inset shows a blow-up around the a-axis for fields in the ac-plane. Superposed are the frequency predictions from LDA band structure calculations, for both the orthorhombic (thin dashed lines) and the hypothetical cubic (thick solid lines) unit cells | the colour code corresponds to Fig. 3.

We also deduced the effective quasiparticle masses  $m^*$  from the thermal broadening factor  $R_T = X/\sinh X$ ,  $X = 2^2 k_B T m^* / \hbar B$ , by comparing dHvA amplitudes at different temperatures in runs from 50 mK up to 1.1 K. As seen in Fig. 4, we have  $m^* \propto 1/B$  for all orbits and for all field directions assessed, save for the hole orbit of the "jungle gym". Such homogeneous scaling of  $m^*$  with  $B$  is seen in the TB model in two-dimensional metals with a low-lying and with primarily nearest-neighbour interactions. This result also supports our assumption of the effective cubic symmetry, because the FS sheets of a cubic  $d^1$  system are essentially formed from three intersecting cylinders containing the  $d_{xy}$ ,  $d_{xz}$ , and  $d_{yz}$  states respectively, and each has a two-dimensional character. The specific heat deduced from dHvA is 8.6 mJ/moleK, which is in good agreement with the bulk experimental value [23] of 7.3 mJ/moleK and is enhanced over the unrenormalized LDA density of states by about a factor of two.

Although some details in the experimental dHvA spectrum of  $\text{CaVO}_3$  remain yet to be identified and are possibly associated with remnant features of the intrinsic orthorhombic structure, the overall angle dependence of the

dHvA frequencies is altogether well captured by the hypothetical "cubic" TB model, rather than the orthorhombic LDA band calculation.

Our apparently ad hoc assumption that the effective crystal symmetry sensed by the 3d electrons is cubic, may be justified if the gaps in the energy bands that are produced by the orthorhombic distortion are small enough | an effect known as magnetic breakdown (MB) [20]. However, its appearance here seems to be surprising, since the orthorhombic distortion in  $\text{CaVO}_3$  is not small (the buckling of the V-O-V bond angle is 160°).

We hope that our results will inspire further, more detailed electronic structure calculations. It will be interesting to see if a high-resolution LDA calculation will show the small gaps due to the orthorhombic distortion that our results imply, and thereby reproduce the predictions of our tight-binding model. If not, some more exotic explanation of the non-appearance of orthorhombic gaps may be required. Also, while the differences between our tight-binding Fermi surface and the measurements are small, they are systematic. In particular, it can be seen in the lower insert of Fig. 2 that the fit to the surface is clearly worse than the others. The sheet is composed

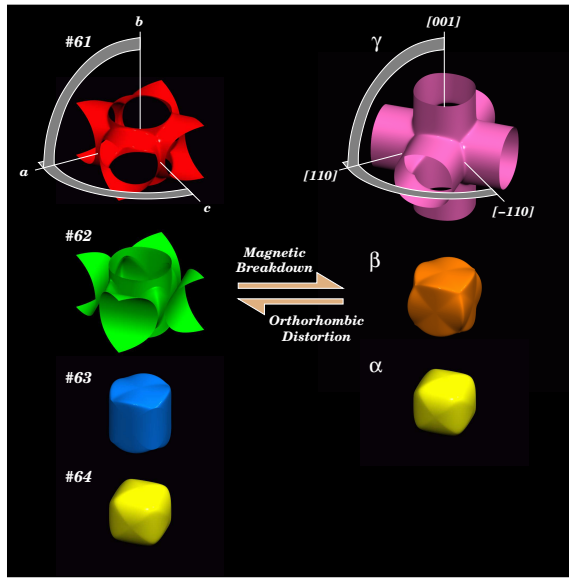


FIG. 3: FS sheets predicted by LDA. The right panels show the FS sheets in a cubic TB to the LDA data, while on the left side these sheets are folded over into the orthorhombic BZ. The field directions in the rotation study are indicated around the surfaces in the top row.

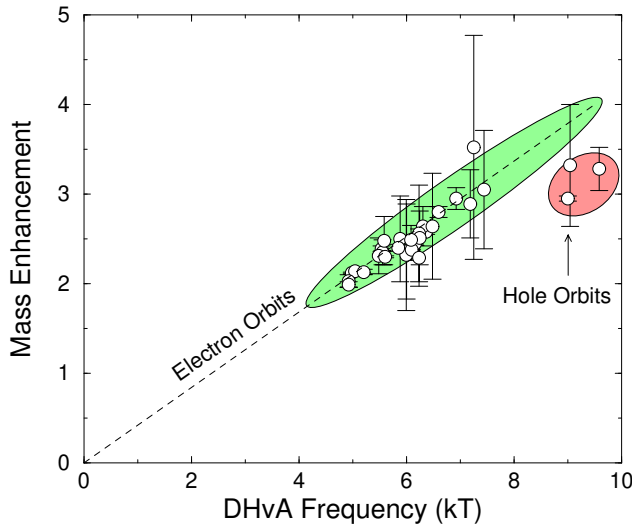


FIG. 4: The ratio of the effective masses to the free electron mass for all observed  $F_{\text{exp}}$  in  $\text{CaVO}_3$  at various field orientations, spaced by about  $15^\circ$  along  $b^* \parallel a^* \parallel c^*$ . The masses scale with the DHVA frequency, except for the 9 kT hole orbit.

of states that are all near an intersection of the three cylinders of the cubic Fermi surface model, so perhaps this is indeed a signature of a non-local interactions, but detailed computational work is clearly required to clarify this, starting with a high-resolution LDA calculation of the electronic structure.

In summary, this first comprehensive investigation of the DHVA effect in a 3d TMO has unraveled the shape of

the FS sheets and thus the electronic structures near the MIT transition in  $\text{CaVO}_3$ . The experimental FS cannot be explained by the LDA band calculation for the intrinsic orthorhombic lattice, but the results are well captured by a hypothetical "cubic" electronic structure. At low energy scales,  $\text{CaVO}_3$  is seen to be a standard metal with moderate mass enhancement, in marked contrast to the strong correlations visible at higher energies. While further efforts are required to comprehend this discrepancy and to gain a quantitative understanding of the origin of the MB effects, this work provides at least a first glimpse of the completely unexplored fermiology near the MIT transition.

We thank D. M. Broun, H. Bando, and W. Y. Liang for their support. We also thank H. Nakotte and M.-H. Jung for sharing their data prior to publication. This work was supported in part by the JST Overseas Research Fellowship and the UK EPSRC.

- 
- [1] J. G. Bednorz and K. A. Müller, Z. Phys. B 64, 189 (1986).
  - [2] J. Orenstein and A. J. Millis, Science 288, 468 (2000).
  - [3] Y. Tokura (ed.), Colossal Magnetoresistive Oxides, Gordon and Breach, London (2000).
  - [4] E. Saitoh et al., Nature 410, 180 (2000).
  - [5] Y. Tokura and N. Nagaosa, Science 288, 462 (2000).
  - [6] N. F. Mott, Metal-Insulator Transitions, Taylor and Francis, London (1990).
  - [7] M. Imada, A. Fujimori and Y. Tokura, Rev. Mod. Phys. 70, 1039 (1998).
  - [8] I. H. Inoue et al., Physica B 194 1067 (1994).
  - [9] A. Fukushima et al., J. Phys. Soc. Jpn. 63 409 (1994).
  - [10] N. Shirakawa et al., J. Phys. Soc. Jpn. 64 4824 (1995).
  - [11] I. H. Inoue et al., Phys. Rev. B 58, 4372 (1998).
  - [12] I. H. Inoue et al., Phys. Rev. Lett. 74, 2539 (1995).
  - [13] K. Morikawa et al., Phys. Rev. B 52, 13711 (1995).
  - [14] M. J. Rozenberg et al., Phys. Rev. Lett. 76, 4781 (1996).
  - [15] H. Makino et al., Phys. Rev. B 58, 4384 (1998).
  - [16] K. Maiti et al., Europhys. Lett. 55, 246 (2001).
  - [17] L. Taillefer and G. G. Lonzarich, Phys. Rev. Lett. 60, 1570 (1988).
  - [18] J. M. Luttinger, Phys. Rev. 119, 1153 (1960).
  - [19] More technically, the self-energy  $\Sigma(k; \omega)$  has to be  $k$ -dependent. This is usually ignored in theories of the MIT, but it seems plausible that as screening breaks down on the verge of the MIT such a  $k$ -dependence could arise.
  - [20] D. Shoenberg, Magnetic Oscillations in Metals, Cambridge University Press, Cambridge (1984).
  - [21] O. Gunnarsson and B. I. Lundqvist, Phys. Rev. B 13, 4274 (1976).
  - [22] D. D. Koelling and B. N. Harmon, J. Phys. C: Solid State Phys. 10, 3107 (1977).
  - [23] I. H. Inoue, Researches of the Electrotechnical Laboratory 986, 1 (1999). (available at <http://www.etl.go.jp/en/results/researches/researches986-e.htm>)